

THE XMM-NEWTON BRIGHT SERENDIPITOUS SOURCE SAMPLE (XMM-NEWTON BSS)

R. Della Ceca¹, T. Maccacaro¹, A. Caccianiga¹, P. Severgnini¹, X. Barcons², D. Barret³, F. Carrera²,
G. Hasinger⁴, R.G. McMahon⁵, C. Motch⁶, W. Pietsch⁴, M.J. Page⁷, S. Rosen⁷, A. Schwobe⁸,
M.G. Watson⁹, N.A. Webb³, D.M. Worrall¹⁰, and H. Ziaeeepour⁷

¹Osservatorio Astronomico di Brera, via Brera 28, 20121, Milano, Italy

²Instituto de Física de Cantabria (CSIC-UC), 39005 Santander, Spain

³Centre d'Etude Spatiale des Rayonnements, 9 Avenue du Colonel Roche, 31028 Toulouse Cedex 04, France

⁴Max-Planck-Institut für Extraterrestrische Physik, Postfach 1312, 85741 Garching, Germany

⁵Institute of Astronomy, Madingley Road, Cambridge CB3 0HA, UK

⁶Observatoire Astronomique de Strasbourg, 11 rue dell'Université, 67000 Strasbourg, France

⁷Mullard Space Science Laboratory, UCL, Holmbury St Mary, Dorking, Surrey RH5 6NT, UK

⁸Astrophysikalishes Institut Potsdam, An der Sternwarte 16, 14482 Potsdam, Germany

⁹Department of Physics and Astronomy, University of Leicester, LE1 7RH, UK

¹⁰Department of Physics, University of Bristol, Royal Fort, Tyndall Avenue, Bristol, BS8 1TL, UK

ABSTRACT

The XMM-Newton Survey Science Center is constructing a large (~ 1000 sources) and complete sample of bright serendipitous XMM-Newton sources at high galactic latitude, so as to allow both the discovery of sources of high individual interest as well as statistical population studies. The sample, known as “The XMM-Newton Bright Serendipitous Source Sample” (XMM-Newton BSS), has a flux limit of $\sim 10^{-13}$ erg cm⁻² s⁻¹ in the 0.5–4.5 keV energy band and will be fundamental in complementing other medium and deep survey programs (having fluxes 10 to 100 times fainter) in order to: a) characterize the X-ray sky and its constituents, b) understand the evolution of the population selected and c) define statistical identification procedures to select rare and interesting populations of X-ray sources (e.g. high z clusters of galaxies, BL Lacs, type 2 QSOs, etc.). We discuss here the scientific rationale and the details of the project and we present some preliminary results.

Key words: Missions: XMM-Newton – X-rays: general – Galaxies: Active

The XMM-Newton Survey Science Center (SSC)¹ is assembling a large (about 1000 sources) sample of bright serendipitous XMM-Newton sources at high galactic latitude ($|b| > 20^\circ$), following well defined criteria (completeness, representativeness, etc..) so as to allow both a detailed study of sources of high individual interest as well as statistical population studies.

The sample, known as “The XMM-Newton Bright Serendipitous Source Sample” (XMM-Newton BSS), is designed to have a flux limit of $\sim 10^{-13}$ erg cm⁻² s⁻¹ in the 0.5–4.5 keV energy band. The major scientific goals of this project are to study the mix of different kinds of AGN, and the cosmological evolution of clusters of galaxies.

AGN are expected to be the most numerous class of X-ray sources. The majority of the XMM-Newton BSS sources will have enough statistics (hundreds of counts) to allow X-ray spectral investigations (see e.g. Della Ceca et al. 2000 for the discovery of a Type 2 AGN from X-ray data only). Such X-ray spectral information is fundamental to determine, source-by-source, the amount of metal absorption, the spectral shape, and the presence of reprocessed features (e.g. FeK line). Moreover, at the X-ray limiting flux of the XMM-Newton BSS sample the optical counterparts of the X-ray sources have magnitudes bright enough to allow relatively high-quality optical and near-infrared spectroscopy even with a 4 meter class telescope. X-ray data, combined with optical and near-infrared spectroscopic information, will allow us to investigate the poorly understood relationships (e.g., Maiolino et al. 2001) between narrow- and broad-line AGN in the optical regime, and absorbed and unabsorbed AGN in the X-ray regime.

1. INTRODUCTION AND SCIENTIFIC RATIONALE

X-ray selection provides a well-proven and efficient mean of finding some of the astrophysically most interesting and energetic objects in the Universe, like Active Galactic Nuclei (AGN) and clusters of galaxies.

¹ The XMM-Newton SSC is an international collaboration involving a consortium of several institutions. The XMM-Newton SSC was appointed by ESA to exploit the XMM-Newton serendipitous detections for the benefit of the international scientific community (Watson et al. 2001). See <http://xmmssc-www.star.le.ac.uk> for a full description of the program and the Barcons et al., contribution at this meeting for an updated status of the XMM-Newton XID program.

The completeness of our sample should place our investigations on firm and solid statistical ground. The large area covered by the XMM BSS will allow us also to investigate in detail rare source population (e.g. the long sought type 2 QSOs).

Another crucial issue for cosmology is the evolution of the XLF of clusters of galaxies. Early claims of a negative evolution with redshift are still being tested and refined. For example, the ROSAT results from the RDCS survey (e.g. Rosati et al. 1998; Borgani et al. 2001) show that the negative evolution, if any, is mostly concentrated on the high luminosity ($L_x > 5 \times 10^{44}$ erg s $^{-1}$) part of the XLF. About 120 (in case of negative evolution) and 160 (in case of no evolution) clusters are expected in the XMM-Newton BSS. The largest discrepancy is on the predicted number of high-luminosity ($L_x > 5 \times 10^{44}$ erg s $^{-1}$) systems: ~ 45 are expected in the no evolution case while ~ 15 are expected in the negative evolution case. These numbers, although indicative, illustrate the power of the XMM-Newton BSS as a tool to solve a long-standing problem of the modern physical cosmology. Medium and deep surveys, covering a smaller area of the sky, will sample more efficiently the low luminosity part of the XLF which is already well sampled by the RDCS and for which no strong evidence of cosmological evolution is found (e.g. Rosati et al. 1998). We stress here that the search for rare high-luminosity clusters is best done in shallow surveys covering a large area, such as the XMM-Newton BSS.

When combined with the results from other XMM-Newton medium and deep survey programs (in the same energy band, e.g. AXIS, Barcons et al. 2002; or in different energy selection bands, e.g. HELLAS2XMM - Baldi et al. 2002; Hasinger et al. 2001) the XMM-Newton BSS will extend the baseline for all evolutionary studies (as e.g. the AGN and cluster of galaxies luminosity function) as well as it will allow us to investigate selection effects in the source population due to the used energy selection band. The importance of a large baseline in luminosity and redshift has been already shown by Miyaji et al. (2000) who have combined several surveys of different depth and solid angle carried out with ROSAT to investigate in deeper detail than previously possible the cosmological properties of the AGN population.

An important part of our work with the XMM-Newton BSS will be to define statistical identification procedures to select rare and interesting populations of X-ray sources, enabling the application of these procedures to the vast amount of XMM-Newton serendipitous data that will be accumulated during the lifetime of the mission.

This paper is organized as follows. In section 2 we describe the strategy used to define the source sample. Preliminary results from this project are presented in Section 3, while the summary and conclusions are reported in Section 4.

2. SURVEY STRATEGY

The bright catalogue is designed to contain about 1000 sources with an X-ray flux limit in the 0.5–4.5 keV energy band of $\sim 10^{-13}$ erg s $^{-1}$ cm $^{-2}$. The size of the sample is dictated by the need to reveal and to characterize statistical properties also for minority populations (e.g. high- z clusters of galaxies, BL Lacs objects etc.).

2.1. WHY THE 0.5-4.5 KEV ENERGY BAND ?

The choice of the 0.5–4.5 keV energy band is motivated by the desire to avoid the very soft photons (minimizing non-uniformities introduced by the different values of Galactic absorbing column densities along the line of sight) and by the need of compromising between a broad passband (to favour throughput) and a narrow passband (to minimize non-uniformities in the selection function due to different source spectra). Furthermore in the 0.5–4.5 keV band XMM-Newton has the highest throughput.

2.2. WHICH PRIMARY SELECTION CAMERA?

We have decided to use only data from the EPIC MOS2 detector to define the source sample. The main reasons for this choice are:

1. unlike the EPIC pn, the EPIC MOS detectors have a circular symmetry that simplifies the analysis of the field. For example, in the case of the EPIC MOS detectors the source target is, in the large majority of the observations, in the central chip;
2. the PSF in the 2 EPIC MOSs is narrower than the PSF in the EPIC pn. In particular, the EPIC MOS2 has the narrowest PSF (FWHM $\sim 4.4''$ and HEW $\sim 13.0''$ at 1.5 keV, see Ehle et al. 2001). As a comparison, the EPIC pn PSF has FWHM $\sim 6.6''$ and HEW $\sim 15.2''$;
3. the dead spaces between the EPIC MOS chips are narrower than the gaps in the EPIC pn detector, simplifying source detection and analysis and maximizing the search area;
4. unlike with the EPIC pn camera, we can use the EPIC MOS2 observations in large- and small-window mode excluding the area occupied by the central chip. Since $\sim 30\%$ of the observations have been performed in window mode, retaining these observations will maximize the searched area, speeding up the creation and definition of the source sample.

The major disadvantage of the EPIC MOS2 camera when compared to the EPIC pn camera is the reduced sensitivity. The effective area of EPIC MOS is smaller than that of EPIC pn, and this is particularly true at high ($E > 5$ keV) and low ($E < 1.5$ keV) energies (note that for the selection band adopted, 0.5–4.5 keV, only the reduced effective area at $E < 1.5$ keV is important). However, since the sample contains relatively bright sources, and considering a minimum exposure time of 5000 s (see below) this

lower efficiency **does not affect the source selection**. Obviously, once the source is detected and included in the sample, additional information using data from the EPIC MOS1 and pn detectors can be collected in order to increase the statistics for the X-ray spectra and morphology analysis.

2.3. CRITERIA FOR FIELD SELECTION

Not all the available EPIC MOS2 pointings are adequate for producing the bright source catalogue. We have defined a set of selection criteria in order to avoid problematic regions of the sky, to maximize the availability of ancillary information at other frequencies (i.e. optical and radio) and to speed up the optical identification process. The fields will be thus selected on the basis of the following criteria:

1. availability to SSC (XMM-Newton fields with PI granted permission² plus XMM-Newton public fields);
2. high Galactic latitude ($|b| \geq 20^\circ$) to avoid crowded fields, to obtain a relatively “clean” extragalactic sample and to have magnitude information for the optical counterparts from the Digital Sky Survey (DSS) material (the Automated POSS Machine - APM - catalogue is almost complete for $|b| \geq 20^\circ$);
3. galactic absorbing column density along the line of sight less than 10^{21} cm^{-2} , to minimize non-uniformities introduced by large values of the Galactic N_H ;
4. exclusion of fields centered on bright and/or extended X-ray targets and/or containing very bright stars. In the first case the effective area of sky covered and the actual flux limit are difficult to estimate correctly, making the derivation of the sky-coverage more uncertain; in the latter case the search for the optical counterpart of the X-ray sources could be very difficult or even impossible due to the presence of the bright star;
5. good time interval (GTI) exposure $> 5\text{ks}$. With this constraint all the sources with a count rate (0.5 - 4.5) $\text{keV} \geq 0.01 \text{ cts/s}$ will be detectable across the whole field of view considered ensuring a flat sensitivity;
6. finally, we have also excluded EPIC MOS2 pointings suffering from a high background rate (i.e. accumulated during particle background flares).

Note that we have also considered the EPIC MOS2 observations in large- and small-window mode satisfying the criteria discussed above; in these cases we exclude the central chip from the investigated area but use the area covered from the other six CCDs.

2.4. SOURCE DETECTION

The EPIC MOS2 observations appropriate for this project have been processed through the pipeline processing sys-

² This restriction of course only applies during the proprietary period of the XMM-Newton observations.

tem, using tasks from the XMM-Newton Science Analysis Software. Full details about the pipeline processing system, the pipeline products as well as the source searching procedures, flux measurements, etc.. can be found in Watson et al. 2001 and <http://xmmssc-www.star.le.ac.uk>.

2.5. CRITERIA FOR SOURCE SELECTION

Having decided the field-selection criteria, we define here the criteria for the source selection within each EPIC MOS2 field:

1. 0.5–4.5 keV count-rate $\geq 0.01 \text{ cts/s}$. This count-rate, already corrected for vignetting and PSF corresponds, for a source with a power-law spectrum with energy index $\alpha_E=0.9$ (see Section 3.3), to a flux (0.5 - 4.5 keV) of $\sim 7 \times 10^{-14} \text{ erg s}^{-1} \text{ cm}^{-2}$;
2. sources with a distance from the EPIC MOS2 center between an inner radius (R_{in}) and an outer radius (R_{out}). R_{in} depends on a) the actual size and brightness of the target and b) on the window mode. R_{in} ranges between 0 (e.g. survey fields with no “target”) and 8 arcmin (bright/extended X-ray sources and/or large- and small-window mode). In this way the area of the detector “obscured” by the presence of the target and/or not exposed is excluded from the analysis. R_{out} is, for the large majority of the fields, equal to 13 arcmin;
3. we have also excluded the sources too close to the edges of the field of view or to the gaps between the CCDs. We note that these sources could have either the flux and/or the source centroid affected by the proximity to the edges and/or the gaps, and therefore could represent a problem in the subsequent analysis and/or interpretation of the data. The excluded area has been taken into account in the computation of the sky coverage;
4. finally, in order to guarantee that all the sources in the catalogue are truly serendipitous we have excluded the target and the sources physically related to the target.

3. PRELIMINARY RESULTS

At the time of this writing (January, 2002) 104 suitable XMM-Newton fields have been already analyzed and a first sample of 185 sources selected. Some general considerations, tested and verified using this initial sample, are in order:

- the majority of the X-ray sources have enough statistics (hundreds of counts when data from EPIC MOS1 and pn are also considered) to allow X-ray studies in terms of energy distribution, source extension and flux variability;
- the optical counterpart, for the large majority (85% - 90%) of the objects, has a magnitude above the POSS II limit ($R \sim 21^{mag}$), thus allowing spectroscopic identification at a 4m class telescope. Furthermore, given

- the positional accuracy of XMM-Newton for the bright sources (90% error circle of 2-5 arcsec) and the magnitude of the optical counterparts, only one object needs to be observed to secure the optical identification. Among the blank fields, rare and interesting classes of X-ray sources (e.g. high z clusters of galaxies, BL Lacs, highly absorbed AGN) could be present;
- about 20% of the sources are identified through a literature search (NED, SIMBAD);
 - for all the sources north of -40° radio information is available down to a few mJy level (NRAO VLA Sky Survey, NVSS; Condon et al. 1998). Information at other wavelength, although incomplete will be abundant (e.g. the 2MASS survey, optical colors).

3.1. THE NUMBER-COUNTS RELATIONSHIP

In Figure 1 we show (filled circles) a binned representation of the number-flux relationship, obtained by folding the sky coverage with the flux of each source. As already said, the sky coverage of the XMM-Newton BSS at the flux limit used to define the sample, is flat and up to now ~ 9.1 sq.deg. have been covered. A conversion factor appropriate for a power-law spectral model with energy index equal to 0.9 (see Section 3.3), filtered by an $N_{H_{Gal}} = 3 \times 10^{20}$ cm $^{-2}$, has been used in the conversion between the count rate and the flux [1 cts/s (0.5–4.5 keV) = 7.2×10^{-12} ergs cm $^{-2}$ s $^{-1}$ (0.5–4.5 keV)]. This count rate to flux conversion factor is accurate $\pm 20\%$ for all the energy spectral indices in the range between 0.0 and 2.0 and for all the $N_{H_{Gal}}$ in the range between $\sim 10^{20}$ cm $^{-2}$ and $\sim 10^{21}$ cm $^{-2}$.

Because we are primarily interested in the extragalactic number-flux relationship we have excluded from the computation the sources classified as (or suspected to be) stars. In the same figure we also report a parametric representation (green solid line) of the $\text{Log}N(>S)$ – $\text{Log}S$ obtained by applying the maximum likelihood method to the unbinned data (see Gioia et al. 1990 for details). The fit has been performed from a flux of 7.2×10^{-14} ergs cm $^{-2}$ s $^{-1}$ (the faintest flux) to a flux of $\sim 10^{-12}$ ergs cm $^{-2}$ s $^{-1}$. For fluxes brighter than this limit we may not be complete since most of the “bright” X-ray sources were chosen as target of the observation and then excluded, by definition, from the survey. However we note that the space density of sources with flux greater than $\sim 10^{-12}$ ergs cm $^{-2}$ s $^{-1}$ is such that fewer than 2 sources are expected given the sky coverage area.

The $\text{Log}N(>S)$ – $\text{Log}S$ can be described by a power-law model $N(>S) = K \times S^{-\alpha}$ with best-fit value for the slope $\alpha = 1.65 \pm 0.19$ (68% confidence interval). The normalization K is determined by rescaling the model to the actual number of objects in the sample and, in the case of the “best” fit model, is equal to $K = 2.21 \times 10^{-21}$ deg $^{-2}$.

The red dashed line represents the extragalactic ROSAT (0.5 – 2.0 keV) $\text{Log}N(>S)$ – $\text{Log}S$ adapted from Hasinger

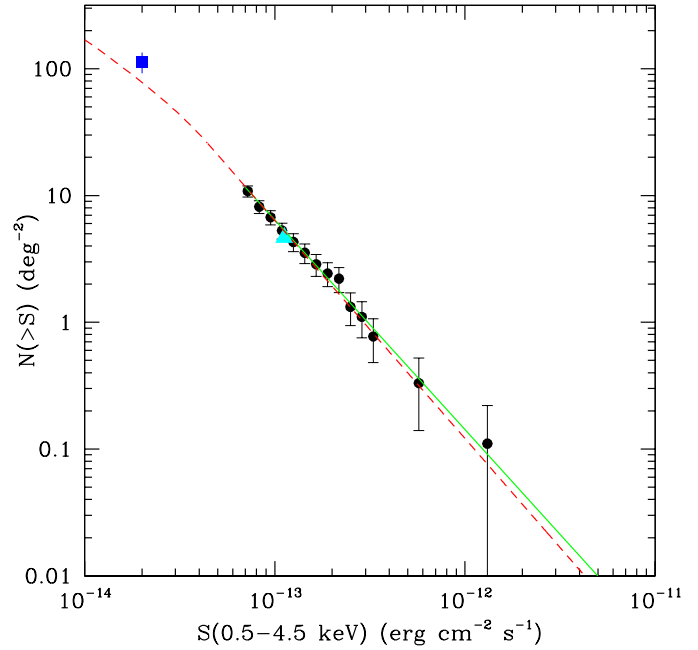


Figure 1. The extragalactic number-flux relationship obtained using the XMM-Newton BSS sample assembled so far (binned representation: black filled circles). The $\text{Log}N(>S)$ – $\text{Log}S$ is well described by a power-law model having a slope equal to 1.65 ± 0.19 (green solid line). In the same figure we have also reported the ROSAT (0.5 – 2.0 keV) $\text{Log}N(>S)$ – $\text{Log}S$ (dashed red line) and the EMSS (0.3–3.5 keV) extragalactic number density (sky-blue triangle) both converted to the 0.5–4.5 keV energy band using a power-law spectral model having $\alpha_E = 0.9$. The blue filled square at $S \simeq 2 \times 10^{-14}$ ergs cm $^{-2}$ s $^{-1}$ represents the extragalactic surface density obtained by the XMM-Newton AXIS Medium Survey team (Barcons et al., 2002).

et al. 1998 and converted to the 0.5–4.5 keV energy band using a power-law spectral model having $\alpha_E = 0.9$. The sky-blue filled triangle at $S \simeq 1 \times 10^{-13}$ ergs cm $^{-2}$ s $^{-1}$ represents the extragalactic number density at the flux limit of the EMSS Gioia et al. 1990 converted from the original (0.3–3.5 keV) to the 0.5–4.5 keV energy band using the same spectral model as before. Finally, the blue filled square at $S \simeq 2 \times 10^{-14}$ ergs cm $^{-2}$ s $^{-1}$ represents the extragalactic surface density obtained from the XMM-Newton AXIS Medium Survey team in the same energy range of the XMM-Newton BSS (Barcons et al. 2002).

As the figure clearly shows, a very good agreement with previous and new results is obtained assuring us about data analysis and selection. Consistent results are also obtained from a comparison with the HELLAS2XMM survey (Baldi et al. 2002).

3.2. OPTICAL IDENTIFICATION AND CLASSIFICATION

The XMM-Newton BSS sample assembled so far is composed of 185 sources. Up to now 59 source have been spectroscopically identified; 39 of these identifications come from the literature (NED, SIMBAD) while 20 from the XMM-Newton XID AXIS project (Barcons et al. 2002). The optical breakdown is the following: 30 broad line AGN (QSOs/Seyfert 1), 3 type 2 AGNs, 1 optically “normal” galaxy, 5 clusters of galaxies, 1 BL Lac object and 19 stars. However we stress that this sample of identified objects is probably not representative of the whole population. A flavour of the dominant X-ray source population in the 0.5–4.5 keV energy range at an X-ray flux limit of $S \simeq 2 \times 10^{-14}$ ergs cm⁻² s⁻¹ may be obtained from the almost complete (93%) spectroscopic identification of a small sample of 29 X-ray sources selected from two XMM-Newton fields studied in the AXIS project (Barcons et al. 2002).

3.3. SPECTRAL PROPERTIES

A “complete” spectral analysis for all the sources in the bright sample (using data from the two EPIC MOSs and the EPIC pn) is in progress. In the meantime and in order to gain X-ray spectral information we present here a “Hardness Ratio” analysis of the single sources using only EPIC MOS2 data; this latter method is equivalent to the “color-color” analysis largely used at optical wavelengths.

We have used the hardness ratios as defined from the XMM-Newton pipeline processing:

$$HR2 = \frac{C(2 - 4.5 \text{ keV}) - C(0.5 - 2 \text{ keV})}{C(2 - 4.5 \text{ keV}) + C(0.5 - 2 \text{ keV})}$$

and

$$HR3 = \frac{C(4.5 - 7.5 \text{ keV}) - C(2 - 4.5 \text{ keV})}{C(4.5 - 7.5 \text{ keV}) + C(2 - 4.5 \text{ keV})}$$

where $C(0.5-2 \text{ keV})$, $C(2-4.5 \text{ keV})$ and $C(4.5-7.5 \text{ keV})$ are the count rates ³ in the 0.5–2, 2–4.5 and 4.5–7.5 keV energy bands, respectively. We have not used here HR1 which is defined using $C(0.15-0.5 \text{ keV})$ and $C(0.5-2 \text{ keV})$ energy band since the count rate in the (0.15–0.5 keV) energy band is a strong function of the Galactic absorbing column density along the line of sight. Note that the effect on HR2 and HR3 due to the different N_{HGal} for the objects in the sample (which range between $\sim 10^{20}$ to 10^{21} cm⁻²) is completely negligible.

In Figure 2 we show the HR2 as a function of the count rate in the (0.5 – 4.5) keV energy band. On the top, we have reported the flux scale computed assuming a conversion factor appropriate for $\alpha_E = 0.9$, which is the mean energy spectral index of the “extragalactic”

sample in the 0.5–4.5 keV energy band (see below). We have used different colors to mark the spectroscopically identified and classified objects. It is worth noting that a) all but 2 ($\sim 90\%$) of the sources classified as stars have an HR2 less than -0.8 and b) none of the X-ray sources identified so far with extragalactic objects have HR2 below -0.8 . If we assume a simple Raymond-Smith thermal model, $HR2 \leq -0.8$ corresponds to temperatures below ~ 1.5 keV, in very good agreement with the stellar identification. This is a first nice result on the statistical broad band properties of the sample; this criterion, if confirmed from better statistics, could be used to select (or exclude depending on the scientific goal) the stars from the XMM-Newton source database. We are at the moment investigating the combination of this criteria with the usual X-ray to optical flux ratio.

No obvious trend of the source spectrum as a function of the count rate is clearly visible. If we exclude the objects classified as stars the weighted average is $HR2 = -0.58 \pm 0.02$ corresponding to $\alpha_E = 0.9 \pm 0.1$. For comparison the weighted average of the sources classified as Broad Line AGN, clusters of galaxies and unidentified objects is $HR2 = -0.56 \pm 0.02$, $HR2 = -0.52 \pm 0.1$ and $HR2 = -0.58 \pm 0.03$, respectively. Two of the three sources identified as Narrow Line AGN seem to have an energy spectral index flatter than that of the cosmic X-ray background ($\alpha_E = 0.4$ corresponding to $HR2 = -0.39$); on the contrary none of the X-ray sources identified as Broad Line AGN seem to have a spectra flatter than $\alpha_E = 0.4$. Finally among the unidentified sources about 13% seem to be described by an energy spectral index below $\alpha_E = 0.4$.

In Figure 3 we report HR3 as a function of the count rate in the (0.5 – 4.5) keV energy band (symbols and flux scale on the top are as in Figure 2). This hardness ratio is much noisier since many of the sources are detected with poor statistics (or even undetected) in the 4.5–7.5 keV energy band. No separation between the different classes of X-ray sources is clearly visible although the large errors could prevent us from finding possible differences. With the same caveat, no obvious trend of the source spectra as a function of the count rate is clearly visible; the median HR3 of the “extragalactic” population is $HR3 \sim -0.57$ corresponding to $\alpha_E \sim 0.7$.

Combining the information on HR2 and HR3 we can study the broad band (0.5–7.5 keV) spectral properties of the sample as well as the selection function of the XMM-Newton BSS. In Figure 4 we report the position of the unidentified objects in the HR2-HR3 plane. Because of the large errors on HR3 for some of the sources, we have plotted here only the 85 unidentified sources with at least 100 net counts in the 0.5–4.5 keV energy band. We have also reported in this figure the expected HR2 and HR3 values for a simple absorbed power-law model as a function of α_E and N_H . In this simple model the absorption has been assumed at $z \sim 0$; for comparison the red line corresponds to an absorption with $N_H = 10^{22}$ cm⁻² at $z=1$. Finally in

³ Note that the count rates have been computed using the exposure-map in each energy band, so that energy dependent vignetting is approximately corrected.

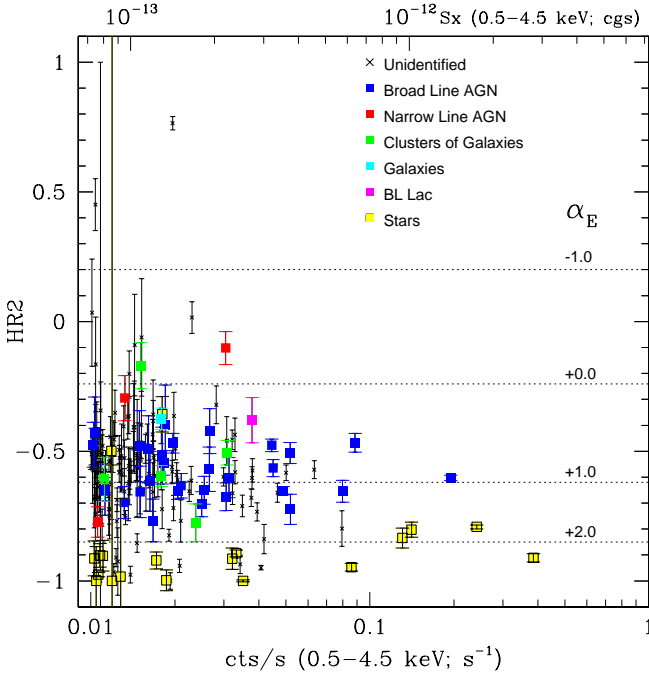


Figure 2. HR2 vs. EPIC MOS2 count rate in the (0.5–4.5) keV energy band for the 185 objects assembled so far, compared with the HR2 expected from a non-absorbed power-law model with α_E ranging from -1 to 2 ($S_E \propto E^{-\alpha_E}$). For comparison the energy spectral index of the CXB ($\alpha_E = 0.4$) corresponds to $HR2 = -0.39$. The flux scale on the top has been computed assuming a conversion factor appropriate for $\alpha_E = 0.9$, the mean energy spectral index of the “extragalactic” sample in the (0.5–4.5) keV energy band. We have used different colors to mark the identified objects.

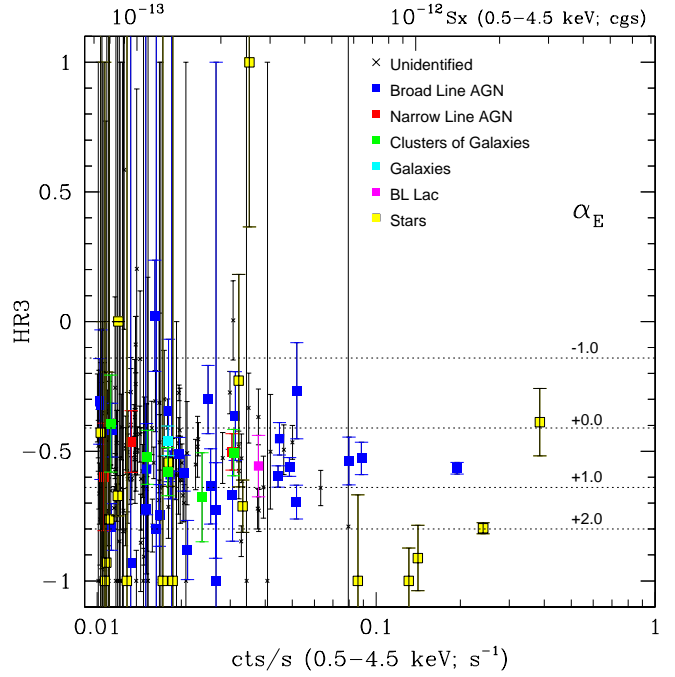


Figure 3. HR3 vs. EPIC MOS2 count rate in the (0.5–4.5) keV energy band for the 185 objects assembled so far, compared with the HR3 expected from a non-absorbed power-law model with α_E ranging from -1 to 2 ($S_E \propto E^{-\alpha_E}$). For comparison the energy spectral index of the CXB ($\alpha_E = 0.4$) corresponds to $HR3 = -0.51$. The flux scale on the top has been computed assuming a conversion factor appropriate for $\alpha_E = 0.9$, the median energy spectral index of the sample in the (0.5–4.5) keV energy band. We have used different colors to mark the identified objects.

Figure 5 we report the position of the identified objects in the HR2 - HR3 plane.

Useful information can be extracted by comparing the position of the sources with the “locus” expected from a simple absorbed power-law model. The “bulk” of the sources are strongly clustered in the region where “unabsorbed” objects are expected. There are very few objects with hardness ratios consistent with those expected from an absorbed power-law model having N_H (at $z=0$) in the range between $10^{21.5}$ and 10^{23} cm^{-2} (four more objects are present in this area if we consider also the unidentified sources with less than 100 counts). It is too early to speculate whether the paucity of these objects is due to selection effects (energy band, flux limit, etc..) or it is intrinsic. It will be instructive to compare the results obtained from the XMM-Newton BSS with the results obtained from other samples selected at harder energies e.g. in the 5–10 keV energy range.

Indeed we are able to detect absorbed objects; for example we already have 3 Narrow Line AGN and two of these sources have the hardest spectra amongst the iden-

tified objects, highly suggestive of intrinsic absorption. It is worth noting that the class of “Compton thick” absorbed AGN, which could represent a considerable fraction of the absorbed AGN population (Bassani et al. 1999; Risaliti et al. 1999), could have X-ray spectral properties similar to that expected from unabsorbed AGN (see Della Ceca et al. 1999). Moreover an absorbed AGN at $z=1$ having $N_H \sim 10^{22}$ cm^{-2} should have hardness ratios around the red line reported in Figure 4; at the flux limit of the XMM-Newton BSS this AGN should have an intrinsic X-ray luminosity $\sim 3 \times 10^{44}$ erg s^{-1} i.e. in the type 2 QSOs regime. Therefore, some Type 2 QSOs could be already present among the unidentified sources. For these objects the XMM-Newton BSS will be fundamental since, for many of them, it will be possible to compare their X-ray spectral properties (e.g. presence of Fe lines, spectral slope, etc..) with the optical ones (e.g. presence of broad and/or narrow line, colors etc..).

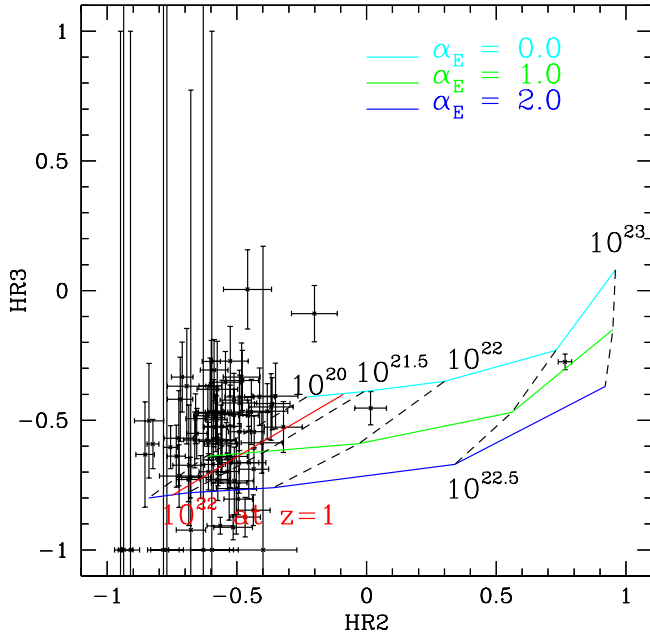


Figure 4. HR2 vs. HR3 for the unidentified objects. For clarity we have reported only the 85 unidentified sources with at least 100 counts in the 0.5–4.5 keV energy band. We have also reported the expected HR2 and HR3 values for an absorbed power-law model as a function of α_E and N_H ; the absorption has been assumed at $z \sim 0$. The red line corresponds to an absorption with $N_H = 10^{22} \text{ cm}^{-2}$ at $z=1$.

4. SUMMARY AND CONCLUSIONS

In this paper we have discussed “The XMM-Newton Bright Serendipitous Source Sample” (XMM-Newton BSS). This sample is designed to contain ~ 1000 sources at high galactic latitude having a flux limit of $\sim 10^{-13} \text{ erg cm}^{-2} \text{ s}^{-1}$ in the 0.5–4.5 keV energy band⁴. The main scientific goals of the project are the study of the mix of the different kind of AGN, the investigation of the cosmological evolution of clusters of galaxies and the definition of a statistical identification procedure to select rare and interesting populations of X-ray sources using the “huge” amount of data that will be accumulated by XMM-Newton in the next few years.

We have discussed the survey strategy with respect to the energy selection band, primary selection camera (EPIC MOS2 detector), criteria for field and source selection.

⁴ Given a density of about 1.8 XMM-Newton BSS source per EPIC MOS2 field we need about 600 suitable EPIC MOS2 data set to build up the sample. At the actual XMM-Newton observation rate we expect to complete the selection and definition of the XMM-Newton BSS sample (~ 1000 sources) in two years.

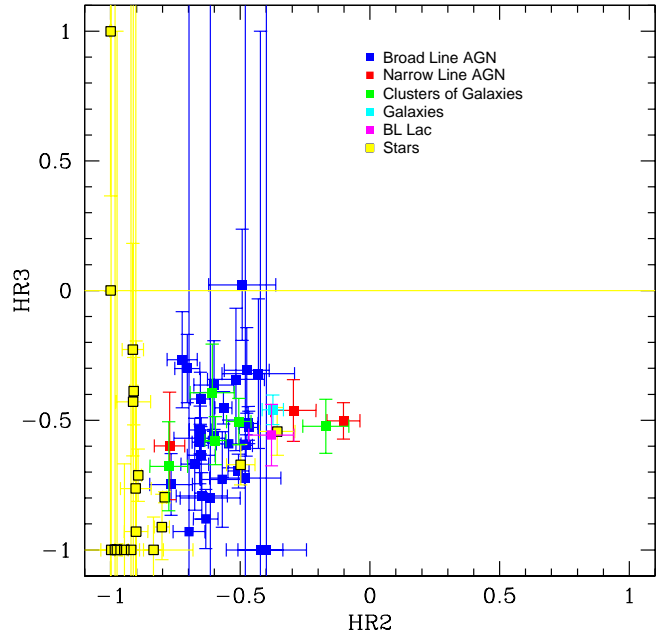


Figure 5. HR2 vs. HR3 for the identified objects. We have used different colors to mark the identified objects.

From the analysis of 104 EPIC MOS2 fields, a first sample of 185 X-ray sources has been selected.

A preliminary analysis indicates that:

- a) the optical counterpart of the majority (85–90%) of these X-ray sources has an optical magnitude above the POSS II limit ($R \sim 21^{mag}$), thus allowing spectroscopic identification on a 4 meter telescope;
- b) given the X-ray positional accuracy of such bright sources (2–5 arcsec at the 90% confidence level) and the magnitude of the optical counterpart only one object needs to be observed to obtain the optical identification;
- c) the majority of the X-ray sources have enough statistics (hundreds of counts if data from EPIC MOS1, MOS2 and pn are combined) to allow X-ray studies in terms of energy distributions, source extent and flux variability.

Fifty-nine sources (32% of the sample) have been identified so far. The large majority of the identified objects are broad line AGN (30); we have also found 3 narrow line AGN, 1 optically “normal” galaxy, 5 clusters of galaxies, 1 BL Lac object and 19 stars. However please note that the sample of identified objects is not statistically representative of the full sample.

Using the sample of 185 sources, we have investigated the number-flux relationship, which is well described by a power law model, $N(>S) = K \times S^{-\alpha}$, with best fit value for the slope of $\alpha = 1.65 \pm 0.19$ (68% confidence interval). A very good agreement with previous and new results is obtained making us confident of the correctness of data selection and analysis.

We have investigated the broad band spectral properties of the sample using the hardness ratio method. No obvious trend of the source spectra as a function of the count rate is clearly visible. The average spectra of the “extragalactic” population corresponds to an energy spectral index of $\alpha_E = 0.9$; about 13% of the sources seem to be described by an energy spectral index flatter than that of the CXB ($\alpha_E = 0.4$).

A nice result is the finding of a clear separation, in the hardness ratio diagram, between galactic stars and extragalactic sources.

Using the position of the sources in the hardness ratio diagram we have also discussed the possible composition of the XMM-Newton BSS as a function of intrinsic absorption. Apparently we found very few sources which seem to be described by an absorbed power-law having N_H (at $z=0$) in the range between $10^{21.5}$ and 10^{23} cm^{-2} . To shed light on the CXB modeling it will be important to compare the source composition of this sample with the source composition of complete samples selected at harder energies (e.g. 5–10 keV energy range). On the other hand our sample could contain “Compton thick” local sources and/or high luminosity type 2 AGN. In this respect the XMM-Newton BSS will be, once fully identified, an important tool to investigate and to compare in detail X-ray and optical/infrared spectral properties.

Finally the XMM-Newton BSS will be instrumental to investigating the cosmological evolution properties of clusters of galaxies. Up to now only 5 X-ray sources have been identified as clusters of galaxies. On the basis of known cosmological properties we expect between 120 (in the case of negative evolution) and 160 (in the case of no evolution) clusters of galaxies; the largest discrepancy is on the predicted number of clusters in the high luminosity - high z plane, a region not well sampled yet. An appropriate source detection algorithm for extended sources (e.g. wavelet) is under investigation.

ACKNOWLEDGEMENTS

This work is based partly on observations with XMM-Newton, an ESA Science Mission with instruments and contributions directly funded by ESA Members States and the USA (NASA). The XMM-Newton project is supported by the Bundesministerium für Bildung und Forschung / Deutsches Zentrum für Luft- und Raumfahrt (BMBF/DLR), the Max-Planck Society and the Heidenhain-Stiftung. This research has made use of the NASA/IPAC Extragalactic Database (NED; which is operated by the Jet Propulsion Laboratory, California Institute of Technology, under contract with the National Aeronautics and Space Administration) and of the SIMBAD database (operated at CDS, Strasbourg, France). RDC, TM and AC acknowledge partial financial support by the Italian Space Agency (ASI) and by the MURST (Cofin00-32-36). PS acknowledge partial financial support by the Italian *Consorzio Nazionale per l'Astronomia e l'Astrofisica* (CNAA). XB and FJC acknowledge financial support from the Spanish MCyT under project AYA2000-1690. AS was supported by the DLR under grant 50 OX 9801 3.

REFERENCES

- Baldi, A., Molendi, S., Comastri, A., Fiore, F., Matt, G., & Vignali, C. 2002, *Ap.J.*, 564, 190
- Barcons, X., Carrera, F.G., Watson, M.G., et al., 2002, *A&A*, 382, 522
- Bassani, L., Dadina, M., Maiolino, R., Salvati, M., Risaliti, G., Della Ceca, R., Matt, G., & Zamorani, G. 1999, *Ap.J. Supp.*, 121, 473
- Borgani, S. et al. 2001, *Ap.J.*, 561, 13
- Condon, J. J., Cotton, W. D., Greisen, E. W., Yin, Q. F., Perley, R. A., Taylor, G. B., & Broderick, J. J. 1998, *A.J.*, 115, 1693
- Della Ceca, R., Castelli, G., Braitto, V., Cagnoni, I., & Maccacaro, T. 1999, *Ap.J.*, 524, 674
- Della Ceca, R., Maccacaro, T., Rosati, P., & Braitto, V. 2000, *A&A*, 355, 121
- Ehle, M., et al. 2001, *XMM-Newton Users' Handbook*
- Gioia, I. M., Maccacaro, T., Schild, R. E., Wolter, A., Stocke, J. T., Morris, S. L., & Henry, J. P. 1990, *Ap.J. Supp.*, 72, 567
- Hasinger, G., Burg, R., Giacconi, R., Schmidt, M., Trumper, J., & Zamorani, G. 1998, *A&A*, 329, 482
- Hasinger, G., et al. 2001, *A&A*, 365, L45
- Maiolino, R., Marconi, A., Salvati, M., Risaliti, G., Severgnini, P., Oliva, E., La Franca, F., & Vanzì, L. 2001, *A&A*, 365, 28
- Miyaji, T., Hasinger, G. ., & Schmidt, M. 2000, *A&A*, 353, 25
- Risaliti, G., Maiolino, R., & Salvati, M. 1999, *Ap.J.*, 522, 157
- Rosati, P., Della Ceca, R., Norman, C., & Giacconi, R. 1998, *Ap.J. Lett.*, 492, L21
- Watson, M. G. et al. 2001, *A&A*, 365, L51